Bioorganic & Medicinal Chemistry Letters 21 (2011) 4784–4787

Contents lists available at ScienceDirect

Bioorganic & Medicinal Chemistry Letters

journal homepage: www.elsevier.com/locate/bmcl

3-(3-Phenoxybenzyl)amino-β-carboline: A novel antitumor drug targeting α-tubulin

Reiko Ikeda [a,b], Masaki Kurosawa [a], Takazumi Okabayashi [a], Ayako Takei [a], Masamichi Yoshiwara [a], Tadashi Kumakura [a], Norio Sakai [a], Osamu Funatsu [c], Akinori Morita [d], Masahiko Ikekita [c,d], Yumi Nakaike [a], Takeo Konakahara [a,b,e,*]

[a] Department of Pure and Applied Chemistry, Faculty of Science and Technology, Tokyo University of Science (RIKADAI), Noda, Chiba 278-8510, Japan
[b] Center for Technologies Against Cancer, Tokyo University of Science (RIKADAI), Noda, Chiba 278-8510, Japan
[c] Genome and Drug Research Center, Tokyo University of Science (RIKADAI), Noda, Chiba 278-8510, Japan
[d] Department of Applied Biological Science, Faculty of Science and Technology, Tokyo University of Science (RIKADAI), Noda, Chiba 278-8510, Japan
[e] Research Institute for Science and Technology, Tokyo University of Science (RIKADAI), Noda, Chiba 278-8510, Japan

ARTICLE INFO

Article history:
Received 18 March 2011
Revised 14 June 2011
Accepted 14 June 2011
Available online 22 June 2011

Keywords:
β-Carboline
α-Tubulin
Antitumor drug
Apoptosis

ABSTRACT

3-(3-Phenoxybenzyl)amino-β-carboline **2h** showed extremely-high activity; the IC_{50} value was 0.074 μM. To verify **2h**-induced cell death types, we observed the chromatin condensation, the DNA fragmentation and activated caspase-3 using Hoechst 33342, agarose electrophoresis and western blot, and suggesting **2h**-induced cell death type was apoptosis. Flow cytometry showed that **2h**-treated cell was induced SubG1 cell population after G2/M cell cycle arrest. In addition, using affinity chromatography and peptide mass fingerprinting, we found that interacting protein with this compound was α-tubulin protein.

Many anticancer drugs exert their cytotoxic effects by interfering with cell cycle progression via inhibition or activation of cell cycle regulators, inhibition of DNA replication, induction of DNA damage, or disruption of mitotic spindle formation.[1] In particular, ever since taxol was discovered, spindle microtubules have become a popular target for development of new anticancer drugs.[2,3] Antimicrotubule agents exert their cytotoxic effects during mitosis by interfering with the exchange of tubulin subunits between the microtubules and the free tubulin pool.[4] These drugs inhibit cell proliferation either by increasing microtubule polymerization, for example, taxol, or by promoting microtubule depolymerization, for example, the vinca alkaloids, and thus impede cell division and induce cell death at relatively high concentrations.[5] Many plant-derived products are used to combat malignant tumors. The chemotherapeutic drugs widely used in clinical oncology include anticancer compounds extracted from plants such as taxol and etoposide, or derived from plants alkaloids by simple chemical modification such as the camptothecin (CPT) derivatives topotecan and irinotecan.

β-Carboline has a planar tricyclic ring structure, and the derivatives are widely distributed in nature including in plants, marine life, human tissues, and body fluids.[6] Harman and norharman are very well known. Most of these β-carboline derivatives are endowed with antitumor, anticancer, or intercalating properties. Some of these molecules are benzodiazepine receptors, and their high DNA binding affinity is thought to be partially responsible for their pharmacological activity.[7–10] The interest in clinical application of β-carbolines is based on the physiological effects of these compounds, such as inhibition of cyclin-dependent kinase (CDK),[11] IkappaB kinase (IKK)[12] and topoisomerase I.[9] However, an optimal structure of β-carboline derivatives remains not to be identified. Therefore, in the present study, we synthesized a variety of β-carboline derivatives and evaluated their biological activities.

To determine the cytotoxic effects of synthesized β-carboline derivatives on a human cervical cancer cell line (HeLa S-3), we used the 3-(4,5-dimethylthiazol-2-yl)-2,5-diphenyltetrazolium bromide (MTT) assay (Tables 1–3). Previously, we reported that 3-benzylamino-β-carboline has high-antitumor activity, with an IC_{50} value of 0.11 μM.[13] On the other hand, Boursereau et al. reported that 1-amino-β-carboline has significant anticancer and antiparasite activities.[14]

Therefore, 1-benzylamino-β-carboline derivatives **1a–n** were synthesized from benzaldehyde possessing a methyl, chloro, methoxy, phenoxy, or hydroxy group by reductive amination with 1-amino-β-carboline in moderate to good yields as shown in

* Corresponding author.
E-mail address: konaka@rs.noda.tus.ac.jp (T. Konakahara).

0960-894X/$ - see front matter © 2011 Elsevier Ltd. All rights reserved.
doi:10.1016/j.bmcl.2011.06.061

Table 1
Yields and antitumor activity of 1-benzylamino-β-carbolines in HeLa S-3 cells

Compds	R^2	R^3	R^4	Yield (%)	IC_{50}[a] (μM)
1a	H	H	H	66	24 ± 1
1b	Me	H	H	92	13 ± 1
1c	H	Me	H	74	22 ± 6
1d	H	H	Me	68	26 ± 2
1e	Cl	H	H	68	19 ± 2
1f	H	Cl	H	93	20 ± 4
1g	H	H	Cl	67	18 ± 3
1h	H	Cl	Cl	69	20 ± 1
1i	OMe	H	H	75	15 ± 1
1j	H	OMe	H	77	24 ± 1
1k	H	H	OMe	54	22 ± 2
1l	H	OPh	H	84	2.3 ± 0.1
1m	H	H	OPh	90	15 ± 2
1n	OH	H	H	75	19 ± 1

[a] Drug toxicity was determined by 3-(4,5-Dimethylthiazol-2-yl)-2,5-diphenyltetrazolium bromide (MTT) assay (see Materials and methods). IC50 is drug concentration inhibited the 50% cell growth. Data represent the mean ± S.D. from four independent experiments performed in triplicate experiments.

Table 2
Yields and antitumor activity of 3-benzylamino-β-carbolines in HeLa S-3 cells

Compds	R^2	R^3	R^4	Yield (%)	IC_{50}[a] (μM)
2a	H	H	H	81	0.11 ± 0.01
2b	Me	H	H	82	0.30 ± 0.04
2c	H	Me	H	81	0.21 ± 0.01
2d	H	H	Me	73	6.2 ± 0.2
2e	OH	H	H	79	28 ± 2
2f	H	OH	H	80	0.92 ± 0.10
2g	H	H	OH	79	1.7 ± 0.2
2h	H	OPh	H	85	0.074 ± 0.007
2i	H	H	OPh	73	1.2 ± 0.1
2j	H	OBn	H	69	0.38 ± 0.05
2k	Cl	H	H	89	1.0 ± 0.1
2l	H	Cl	H	89	0.83 ± 0.05
2m	H	H	Cl	74	6.1 ± 1.1
2n	NO_2	H	H	71	14 ± 1
2o	H	NO_2	H	82	>30
2p	CF_3	H	H	75	6.7 ± 0.7
2q	H	CF_3	H	88	3.1 ± 0.4
2r	H	H	CF_3	74	47 ± 10
2s	Ph	H	H	88	3.0 ± 0.4
2t	H	H	Ph	74	>30

[a] Drug toxicity was determined by 3-(4,5-Dimethylthiazol-2-yl)-2,5-diphenyltetrazolium bromide (MTT) assay (see Materials and methods). IC50 is drug concentration inhibited the 50% cell growth. Data represent the mean ± S.D. from four independent experiments performed in triplicate experiments.

Table 3
Antitumor activity of multi-substituted 3-benzylamino-β-carbolines in HeLa S-3 cells

Compds	R^2	R^3	R^4	R^5	R^6	Yield (%)	IC_{50}[a] (μM)
3a	MeO	H	H	H	H	86	0.80 ± 0.06
3b	H	MeO	H	H	H	73	0.79 ± 0.04
3c	H	H	MeO	H	H	82	20 ± 4
3d	MeO	MeO	H	H	H	63	3.2 ± 0.4
3e	MeO	H	MeO	H	H	78	4.8 ± 0.3
3f	MeO	H	H	MeO	H	72	6.1 ± 0.6
3g	MeO	H	H	H	MeO	69	2.3 ± 0.2
3h	H	MeO	MeO	H	H	74	>100
3i	H	MeO	H	MeO	H	73	1.7 ± 0.4
3j	MeO	MeO	MeO	H	H	63	4.0 ± 0.8
3k	H	MeO	MeO	MeO	H	66	0.22 ± 0.03

[a] Drug toxicity was determined by 3-(4,5-Dimethylthiazol-2-yl)-2,5-diphenyltetrazolium bromide (MTT) assay (see Materials and methods). IC50 is drug concentration inhibited the 50% cell growth. Data represent the mean ± S.D. from four independent experiments performed in triplicate experiments.

Scheme 1 and Table 1, according to a usual method (see Supplementary data).

Next, we evaluated the cytotoxicity on a human cervical cancer cell line, HeLa S-3, of compounds **1b**–**n** by MTT method (Table 1).

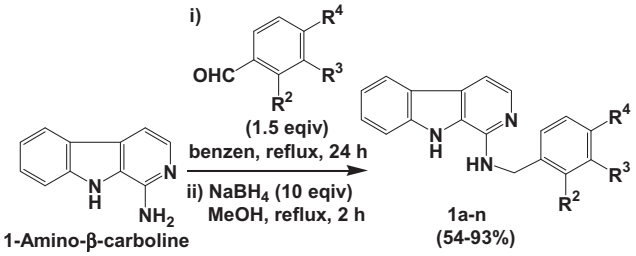

Scheme 1.

The compound **1l** with an OPh group at R^3 showed the highest antitumor activity; the IC_{50} value of **1l** was 2.3 μM. However, the activity of **1l** was lower than that of 3-benzylamino-β-carboline (**2a**), which had an IC_{50} value of 0.11 μM (Table 2). These results suggest that the optimal position for introduction of the benzylamino group is the 3-position of β-carboline nucleolus. Based on this result, we started to optimize the structure of 3-benzylamino-β-carboline to obtain the highest antitumor activity.

3-Benzylamino-β-carboline derivatives **2a–t** were analogously synthesized from 3-amino-β-carboline and benzaldehydes with a methyl, hydroxyl, phenoxy, benzyloxy, chloro, nitro, trifluoromethyl, or phenyl group at R^2–R^4 (Scheme 2). Yields are summarized in Table 2.

Cytotoxicity of **2a**–**t** was evaluated using the MTT assay (Table 2). In general, compounds substituted at R^2 and R^3 showed relatively high antitumor activity. In addition, the antitumor activity of the compounds substitutes at R^3 was higher than that of compounds substituted at R^4. In other words, substitution at the R^4 position reduced the antitumor activity. It was notable that **2h** which has a phenoxy group, had the highest-activity among the compounds **2a**–**t**; the IC_{50} value of **2h** is 0.074 μM. However, the introduction of a NO_2 or CF_3 group significantly reduced the antitumor activity.

Subsequently, in order to determine the influence of poly-substitution on antitumor activity, we synthesized 3-(dimethoxybenyl)amino-, and 3-(trimethoxybenyl)amino-β-carboline derivatives **3d**–**k** by the same method used in the synthesis of **2** as shown in Scheme 3 (see Supplementary data) in moderate to good yields, and evaluated the antitumor activity of these compounds (Table 3). Compared with di-substituted compounds, the tri-substituted derivatives were obtained in slightly lower yield due to steric hindrance. In each case, most of the starting material was recovered together with the desired product. Our efforts to improve the yield of poly-substituted product were unsuccessful. In addition, use of excess aldehyde caused the formation of bis-benzylated compounds.

The 2-, and 3-methoxy derivatives **3a,b** have similarly high antitumor activity, with the IC_{50} values of 0.80 and 0.79 μM, respectively. However, 4-methoxy derivative **3c** shows significantly reduced antitumor activity. These results suggest that the optimal position for monomethoxy-substitution was either the position 2 or 3. To determine the synergistic effect of dimethoxy-substitution on the antitumor activity, the 2,3-, 2,4-, 2,5-, and

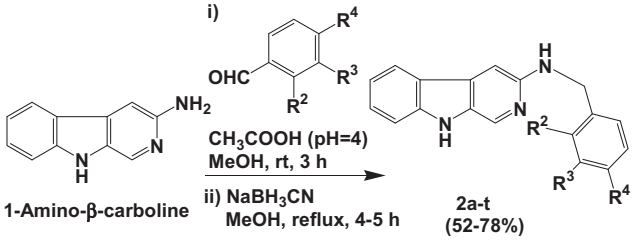

Scheme 2.

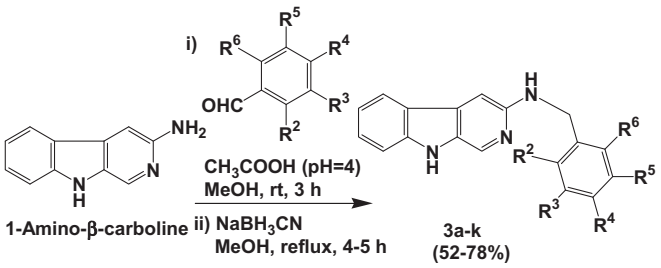

Scheme 3.

2,6-dimethoxy-substituted derivatives **3d**–**g** were synthesized in 63%, 78%, 72%, and 69% yields, respectively (Table 3). The antitumor activities of **3a,b** are very high. However, the antitumor activities of **3d**–**g** are lower than those of **3a**,**b**. Among these compounds, introduction of the 2nd methoxy group at the position 3, 4, 5, or 6 of **3a** slightly decreased the antitumor activity. The 4-methoxy group greatly decreased the antitumor activity of the corresponding compound (see **3c** in Table 3). Especially, introduction of the 2nd 4-methoxy group to **3b** strongly decreases the antitumor activity of the β-carboline derivative **3h**. Although the reason is not clear, 3-(3,4,5-trimethoxybenzyl)amino-β-carboline (**3k**) surprisingly shows the highest antitumor activity among the compounds **3a**–**k**, regardless of its 4-methoxy group; the IC_{50} value of **3k** is 0.22 μM, as shown in Table 3.

Next, we investigated the type of cell death induced. Both chromatin condensation and fragmented nuclei are the classic characteristics of apoptosis. Hoechst 33342 staining showed significant morphological changes in the nuclear chromatin. After treatment of HeLa S-3 cells 0, 150, 300, 1000 nM of **2h**, we observed the nuclear chromatin (Fig. 1). Compared with **2h**-treated cells, untreated cells exhibited less intense nuclear staining. However, a large proportion of **2h**-treated cells exhibited fragmented nuclei.

To verify that cell death occurred via apoptosis, a DNA fragmentation assay was performed. DNA fragmentation is a well known biochemical index of cell apoptosis. After exposure to **2h** for 48 h, the genomic DNA was extracted and analyzed by electrophoresis (Fig. 2). DNA fragmentation was detectable in the cells treated with **2h** (150–1000 nM). Together with fluorescence microscopy analysis, these observations demonstrated that **2h** caused apoptotic cell death.

Caspase-3 is well known as the execution factor of apoptosis. After determining that **2h** induced chromatin condensation and DNA fragmentation, we further investigated the activation of caspase-3 in **2h**-treated cells. As shown in Figure 3, activated caspase-3 was readily detected in cells treated with **2h** for more than 12 h, and it enhanced with the time-dependent. These observations are closely connected with results of the chromatin condensation and DNA fragmentation, suggesting that **2h** induced apoptosis.

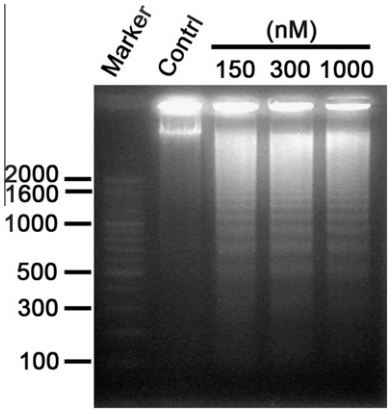

Figure 2. Effect of **2h** on apoptosis induction in HeLa S-3 cells. Cells were treated with **2h** for 48 h. DNA fragmentation was detected by electrophoresis on a 2% agarose gel. Marker; 100 bp ladder.

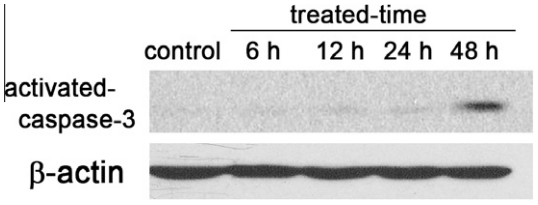

Figure 3. Western blot analysis of activated caspase-3 in HeLa S-3 cells. Cells were treated with **2h** for 6, 12, 24 or 48 h. Control, non-treated cell extract; β-actin was used as internal control.

To examine the effects on cell cycle progression, the cells were exposed to 150 nM of **2h** for 12, 24, 36, or 48 h. After treating for 12 h, the percentage of average G_2/M population at the control cells was 65.92% (see Table 4). For 24 h, this population shifted from G_2/M phase to the mean apoptotic population sub-G_1 phase. These results suggest that **2h** induces apoptosis through G_2/M cells cycle arrest.

Affinity chromatography, which is based on a highly specific biological interaction, such as between antigen and antibody, enzyme and substrate, or receptor and ligand, is used to separate biochemical mixture. In the present study, we sought to identify the

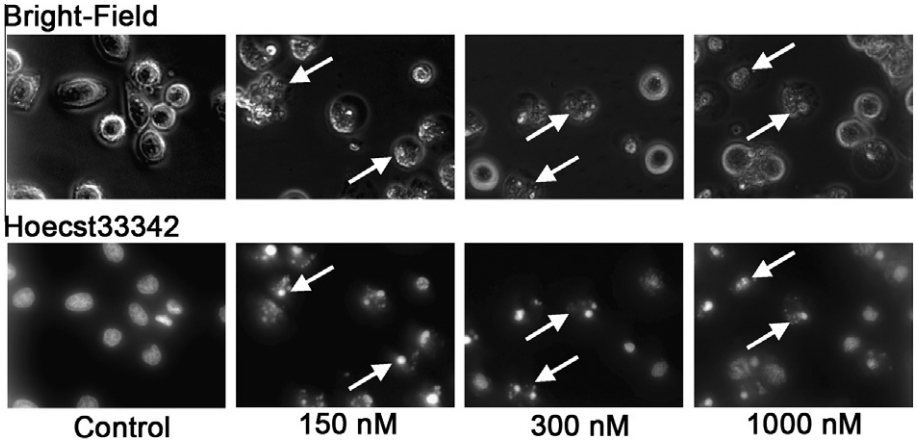

Figure 1. HeLa S-3 cells were treated with **2h** for 48 h. Apoptosis was detected by Hoechst 33342 staining.

Table 4
Effect of **2h** on the distribution of cell-cycle phase in HeLa S-3

Treatment time (h)	SubG$_1$ (%)	G$_1$ (%)	S (%)	G$_2$/M (%)
Control	1.51	56.42	19.62	22.45
12	9.72	8.40	15.38	65.92
24	32.74	21.18	15.93	30.01
36	43.51	18.97	15.62	19.19
48	50.14	18.38	20.16	9.52

HeLa S-3 cells were incubated in the absence (control) or presence of **2h** for 12, 24, 36, or 48 h. Then, the cells were fixed and stained with propidium iodide to analyze DNA content by flow cytometer.

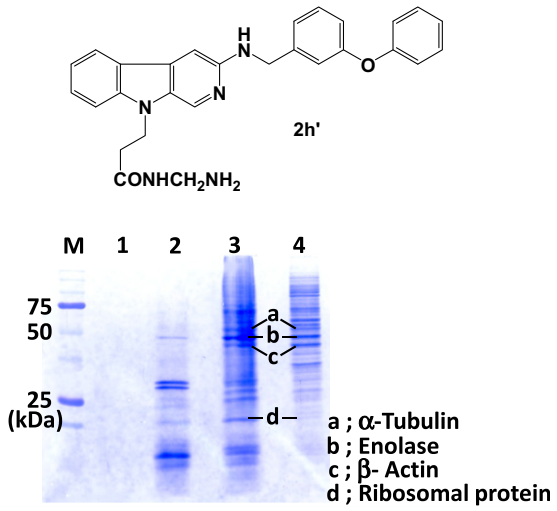

Figure 4. SDS–PAGE analysis of the proteins enriched by affinity chromatography. The ligand (**2h**) was introduced using amino-linker (upper panel). M, size-marker; (1) using NHS-activated sepharose 4 Fast Flow as negative control; (2) solubilized fraction of interacting protein; (3) insolubilized fraction of interacting protein; (4) whole cell lysate.

proteins that interact with **2h**, because it showed the highest antitumor-activity and induced apoptosis. The compound **2h** was used as the ligand on an affinity column, and was immobilized using an amino-linker (Fig. 4, upper panel). The proteins that interacted with the probe **2h**′ were separated by electrophoresis, and subsequently identified using matrix-assisted laser desorption ionization/time of flight-mass spectrometry (MALDI/TOF-MS) (Fig. 4, lower panel, a–d). The proteins shown in a–d were α-tubulin, enolase, β-actin, ribosomal protein, respectively.

Many anticancer drugs are cytotoxic because they interfere with cell cycle progression by inhibition of activation of cell cycle regulation, inhibition of DNA replication, induction of DNA damage, or disruption of mitotic spindle formation.[1] In particular, since taxol was discovered, spindle microtubules have become a popular target for the development of new anticancer drugs.[2,3] These drugs inhibit cell proliferation either by increasing microtubule polymerization, for example, taxol, or by promoting microtubules depolymerization, for example, the vinca alkaloids, thus impeding cell division and inducing cell death at relatively high concentrations.[5] These reports indicate that a delay in progression through mitosis by the induction of aberrant spindle formation might be another mechanism by which anticancer drugs alter cancer cell growth.

In the present study, results of affinity chromatography and peptide mass fingerprinting showed that the protein with the strongest interaction was enolase (Fig. 4). However, inhibition of enolase was probably caused by blockade of the glycolytic system, such as inhibition of the citric acid cycle or the electron transfer system. During preparation for cell division under conditions of energy deficiency, a variety of cell cycle regulators might interfere with the onset of the M phase. Therefore, it does not stand to reason that the cell cycle progressed through the anaphase stage of cell division after DNA replication. Based on the results of the present study, it is reasonable to suggest that α-tubulin might interacting with **2h**. In addition, the flow cytometric analysis demonstrated G$_2$/M-phase arrest of the cell cycle with **2h**. Many microtubule-interfering agents bind to β-tubulin and induce arrest of cell division. Among them, colchicines, vinblastine and taxol have played major roles in practical uses as well as in biochemical studies of microtubules functions. Each of these compounds binds to β-tubulin, however, the protein that interacted with **2h** was α-tubulin. Therefore, **2h** appears to have a different mechanism of action compared with the colchicines, vinblastine and taxol.

The function of α-tubulin in the apoptosis pathway is unclear, and antitumor drugs that are currently in use do not target this protein. For these reasons, the consequences of **2h** effects on α-tubulin remain unclear. Characterization of the relationship between α-tubulin and apoptosis requires identification of molecular/biological mechanisms.

Acknowledgments

This work was partially supported by a Grant-in-Aid for Scientific Research from MEXT, a matching fund subsidy from MEXT 2004–2006 (No. 16550148); a grant for the 'High-Tech Research Center' Project for Private Universities, a matching fund subsidy from MEXT, 2000–2004 and 2005–2007; a Grant from the Japan Private School Promotion Foundation (2008–2009); a Grant-in-Aid for Scientific Research form MEXT, a matching fund subsidy from MEXT 2009–2011 (No. 21590025); and a grant for the Development of strategic Research Center in Private Universities supported by MEXT, Center for Technologies against Cancer (CTC), 2009–2013. We thank Sanae Takasugi, Masaki Takizawa, Takuya Akahane and Taro Nittono (Department of Pure and Applied Chemistry, Faculty of Science and Technology, Tokyo University of Science (RIKADAI)) for experimental work in the synthesis of **3d–k** and MTT assay of **3h–i**.

Supplementary data

Supplementary data associated with this article can be found, in the online version, at doi:10.1016/j.bmcl.2011.06.061.

References and notes

1. Stewart, Z. A.; Westfall, M. D.; Pietenpol, J. A. *Trends Pharmacol. Sci.* **2003**, *24*, 139.
2. Gibbs, J. B. *Science* **2000**, *287*, 1969.
3. Jordan, M. A. *Curr. Med. Chem. Anti-Cancer Agents* **2002**, *2*, 1.
4. Wood, K. W.; Cornwell, W. D.; Jackson, J. R. *Curr. Opin. Pharmacol.* **2001**, *1*, 370.
5. Dumontet, C.; Sikic, V. I. *J. Clin. Oncol.* **1999**, *17*, 1061.
6. Cao, R.; Peng, W.; Wang, Z.; Xu, A. *Curr. Med. Chem.* **2007**, *14*, 479.
7. Hayashi, K.; Nagao, M.; Sugimura, T. *Nucleic Acids Res.* **1977**, *4*, 3679.
8. Ishida, J.; Wang, H. K.; Bastow, K. F.; Hu, C. Q.; Lee, K. H. *Bioorg. Med. Chem. Lett.* **1999**, *9*, 3319.
9. Cao, R.; Peng, W.; Chen, H.; Ma, Y.; Liu, X.; Hou, X.; Guan, H.; Xu, A. *Biochem. Biophys. Res. Commun.* **2005**, *338*, 1557.
10. Zhao, T. J.; Rosenberg, H. C.; Chiu, T. H. *Eur. J. Pharmacol.* **1996**, *306*, 61.
11. Garcia, M. D.; Wilson, A. J.; Emmerson, D. P.; Jenkins, P. R. *Org. Biomol. Chem.* **2006**, *4*, 4478.
12. Castro, A. C.; Dang, L. C.; Soucy, F. S.; Grenier, L. *Bioorg. Med. Chem. Lett.* **2003**, *13*, 2419.
13. Konakahara, T.; Iida, T.; Iwaki, T.; Kumagai, M.; Sakai, N. JP2006321753.
14. Yohan, B.; Iain, C. *Bioorg. Med. Chem. Lett.* **2004**, *14*, 5841.